Advanced Composite Materials
Publication details, including instructions for authors and subscription information:
http://www.tandfonline.com/loi/tacm20

Fatigue behavior and lifetime distribution of impact-damaged carbon fiber/toughened epoxy composites under compressive loading

Toshio Ogasawara [a], Sunao Sugimoto [a], Hisaya Katoh [a] & Takashi Ishikawa [b]

[a] Aerospace Research and Development Directorate, Japan Aerospace Exploration Agency (JAXA), 6-13-1, Osawa, Mitaka-shi, Tokyo 181-0015, Japan

[b] Aerospace Engineering, Graduate School of Engineering, Nagoya University Furoh-Cho, Chikusa-ku, Nagoya-shi, 464-8603, Japan

Published online: 25 Mar 2013.

To cite this article: Toshio Ogasawara, Sunao Sugimoto, Hisaya Katoh & Takashi Ishikawa (2013) Fatigue behavior and lifetime distribution of impact-damaged carbon fiber/toughened epoxy composites under compressive loading, Advanced Composite Materials, 22:2, 65-78, DOI: 10.1080/09243046.2013.768324

To link to this article: http://dx.doi.org/10.1080/09243046.2013.768324

Advanced Composite Materials, 2013
Vol. 22, No. 2, 65–78, http://dx.doi.org/10.1080/09243046.2013.768324

Fatigue behavior and lifetime distribution of impact-damaged carbon fiber/toughened epoxy composites under compressive loading

Toshio Ogasawara[a]*, Sunao Sugimoto[a], Hisaya Katoh[a] and Takashi Ishikawa[b]

[a]*Aerospace Research and Development Directorate, Japan Aerospace Exploration Agency (JAXA), 6-13-1, Osawa, Mitaka-shi, Tokyo 181-0015, Japan;* [b]*Aerospace Engineering, Graduate School of Engineering, Nagoya University Furoh-Cho, Chikusa-ku, Nagoya-shi, 464-8603, Japan*

(*Received 5 October 2012; accepted 17 January 2013*)

This paper presents fatigue lifetime data of impact-damaged carbon fiber/toughened epoxy composites under compressive loading to elucidate the lifetime prediction methodology based on statistical approaches. Drop-weight impact damage was induced to a composite specimen with impact energy of 6.7 J/mm in accordance with ASTM D7136. Postimpact fatigue tests were conducted using a test fixture defined in ASTM D7137 under compression–compression loading ($R = 10$) at room temperature. The maximum compressive stress (S_{min}) was 200, 210, 220, 230, and 240 MPa, and the total number of specimens was 31. The compression-after-impact strength and fatigue lifetime show considerable scattering. This result is apparently derived from the variation in impact damage size. A simple statistical model based on the weakest link theory was proposed for predicting the lifetime of impact-damaged composite laminates. Results show that the experimentally obtained data were confirmed consistently using this model. The ratio between the endurance limit at 10^6 and 10^7 cycles and the initial static strength was estimated as 0.74 and 0.68 as B-basis allowable values.

Keywords: low-velocity impact damage; compression; fatigue; statistical analysis; Weibull distribution

1. Introduction

A major limitation of the design of carbon fiber/epoxy composite structures is the susceptibility of materials to impact damage such as multiple delamination, fiber breakage, and matrix cracking. Low-energy impacts might occur on aircraft structures because of dropped tools, runaway debris, and hailstones. Such impact damage is a potential source of mechanical weakness, particularly under compression loading. Therefore, considerable research effort has been devoted to evaluating compression-after-impact (CAI) behavior. In addition to this, the effects of impact damage on the fatigue behavior of composite laminates should be assessed. The fatigue behavior of impact-damaged carbon fiber/epoxy composite laminates under cyclic compressive loading, that is, CAI fatigue behavior, has been studied since the late 1970s. The CAI fatigue data of CFRP materials were published in related reports.[1–18] A recent report published from the federal aviation administration (FAA) of the US Department of Transportation is especially useful to ascertain fatigue behavior (including CAI fatigue) of

*Corresponding author. Email: ogasat@chofu.jaxa.jp

modern carbon fiber composites.[18] In that article, many CAI fatigue data were reported. Statistical data reduction based on a Weibull distribution function was conducted in detail.

According to data from the literature, it has been understood that the ratios between the endurance limit at 10^6 cycles to the initial static strength turned out to be 0.50–0.75. The delamination growth behaviors were also investigated using nondestructive inspection (NDI) techniques such as ultrasonic C-scanning. Generally, unrealistic fatigue stress (greater than 75% of the static strength) was necessary to observe delamination growth behaviors. Damage growth starts very close to the end of the specimen lifetime with a very high slope.[1,3,6,12] Damage growth under cyclic compressive loading is extremely sensitive to stress, implying that the conventional damage tolerance methodology for aluminum alloys is not applicable for CFRP. Therefore, 'No damage growth' (allowable stress design) is becoming the most common concept for designing composite aircraft structures.[19] For this methodology, the fatigue strength of composite laminates, which have barely visible impact damage (BVID), is extremely important to determine the allowable stress. It is recommended that the B-basis value, which is defined as 95% confidence that 90% of the samples will exceed the allowable stress, is preferred for determining the allowable level for composite materials.[20] Therefore, the B-basis value of fatigue strength of impact-damaged CFRP should be estimated rationally from the fatigue lifetime data to determine the design allowable stress.

However, few reports have described the statistical data reduction of the CAI fatigue behaviors of carbon fiber/epoxy composites except for the FAA report mentioned above.[18] Experimentally obtained results clarifying the fatigue lifetime distribution of impact-damaged carbon fiber/toughened epoxy composite laminates have not been published sufficiently, because they are sensitive information for material suppliers and aircraft manufacturers. Furthermore, a specific statistical data reduction method for postimpact fatigue behavior has not been discussed in detail. Therefore, a standard method based on 'wearout method',[21] which is not specified for CAI fatigue behavior, has been chiefly applied for the data reduction of CAI fatigue behavior until now.

The first objective of this study is to obtain fatigue lifetime data of impact-damaged modern carbon fiber/toughened epoxy composite material (T800S/3900-2B; Toray Industries Inc.) under compressive loading to elucidate the lifetime prediction methodology based on statistical approaches. Drop-weight impact damage is induced to a CFRP specimen, and postimpact fatigue tests are conducted under compression–compression loading ($R = 10$). Furthermore, a simple statistical method for evaluating fatigue lifetime distribution of impact-damaged carbon fiber composites is proposed under the simple assumption of one-to-one correspondence between static strength and fatigue lifetime. Using the statistical method, the B-basis value of the fatigue strength of impact-damaged carbon fiber composites is estimated.

2. Experimental procedures

The material used for this study is high strength carbon fiber/toughened epoxy composite T800S/3900-2B (Toray Industries Inc., Japan). Interleaf layers, which include dispersed thermoplastic polymer particles, are adopted to improve the impact damage resistance. T800S/3900-2B has excellent damage tolerance properties such as impact damage resistance and CAI strength. It is therefore applied to the primary structures of the latest commercial aircraft. The stacking sequence is 32 ply quasi-isotropic laminates ($[45°/0°/-45°/90°]_{4s}$), with thickness of approximately 6 mm. Each specimen has 100 mm width and 150 mm length. Specimens were cut from three 500 × 500 mm square panels (12 specimens/panel).

Low-speed impact loading was applied using a drop-weight type impact tester (model 9250HV; Instron Corp., USA) according to ASTM D7136.[22] The mass of a drop weight,

with an impactor tip radius of 5/8 inches (1.6 cm), was 5.5 kg. The impact energy was set as 6.7 J/mm. The dent depth was approximately 0.2–0.3 mm as shown in Figure 1. The surface crack was propagated along -45° direction, which is transverse direction of the surface layer (45°). The crack length was approximately 25–30 mm. It has been already revealed that the effect of delamination on CAI strength is much more significant than that of surface cracks. BVID is defined as slight damage that might not be detected during heavy-maintenance, general visual inspections using typical lighting conditions from a distance of 5 ft. (1.52 m). The typical dent depth was 0.01 to 0.02 in. (0.254–0.508 mm). Therefore, the damage induced at the center of each specimen is BVID. The delamination diameter was approximately 34 mm, as inspected using ultrasonic C scanning.

Static compressive tests were conducted using a standard fixture in accordance with ASTM D7137 [23] on an electromechanical testing system (250 kN capacity, model 5885; Instron Corp., USA) under a constant displacement rate of 1 mm/min at room temperature. Upper and lower edges were supported rigidly, and both sides of a specimen were supported simply by knife-edge-type linear guides. Nine specimens were examined.

Fatigue tests were conducted on a servo-hydraulic testing rig (500 kN capacity, model 8804; Instron Corp., UK) at 3 Hz frequency with a sinusoidal wave. The test rig and fixture are shown in Figure 2(a). In general, compression is defined as negative stress; therefore, S_{min} is the maximum compressive stress and S_{max} is the minimum compressive stress, respectively. The stress ratio R ($=S_{min}/S_{max}$) was 10, and the S_{min} was 210, 220, 230, and 240 MPa. The total specimens were 31.

Delamination growth behavior was evaluated for a couple of specimens using ultrasonic C-scanning and digital video recorder. The cyclic loading test was interrupted periodically; the specimen was inspected using an ultrasonic C-scanning. The specimen surface was recorded visually using a digital video recorder, and delamination behavior was observed after fatigue testing.

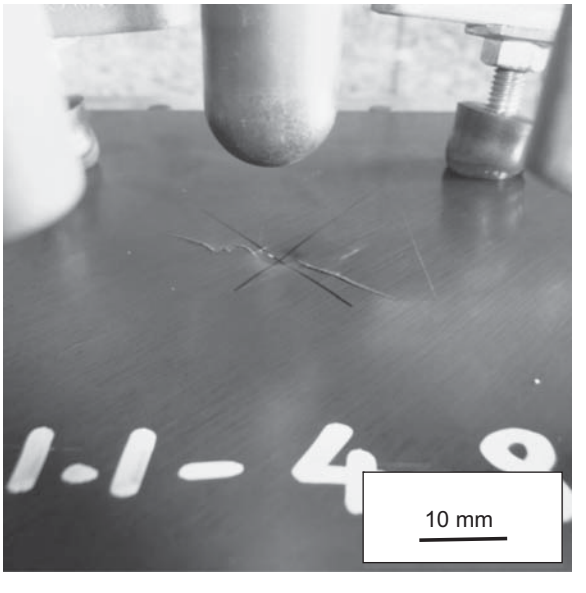

Figure 1. Composite specimen after low-speed impact loading (6.7 J/mm).

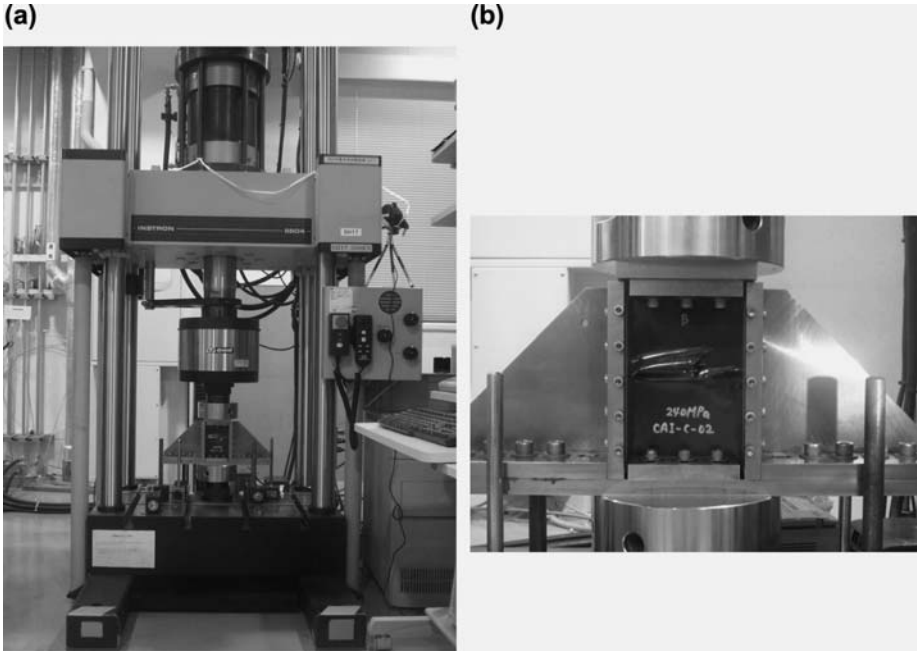

Figure 2. Specimen, fixture, and testing rig used for CAI fatigue testing.

3. Experimental results and discussion

3.1. CAI and NHC strength distribution

The experimentally obtained results of CAI strength are presented in Table 1. Catastrophic compressive failure occurred after the rapid delamination growth in the transverse direction of a specimen, as presented in Figure 2(b). The average CAI strength and coefficient of variation (CV) were, respectively, 272 MPa and 5.4%. The results of compressive strength, which are often designated as non-hole compressive strength (NHC), are also shown in Table 1. The NHC strength values were obtained in accordance with a combined compressive loading method: ASTM D6641.[24] Each NHC specimen has 10 mm width, 3 mm thickness, 120 mm overall length, and 12.7 mm gauge length. The average NHC strength and CV are 583 MPa

Table 1. CAI and NHC strength data.

	CAI strength	NHC strength
Test method	ASTM D7137	ASTM D6641
Specimen dimension (mm)	$100 \times 150 \times$ t6	$12 \times 120 \times$ t3
Average (MPa)	272	583
Standard deviation (MPa)	14.6	10.6
CV (%)	5.4	1.8
Weibull shape parameter (m)	19.4	61.8
Weibull scale parameter (S_0) (MPa)	279	588
Compressive strength data (MPa)	255, 257, 262	566, 573, 579
	263, 273, 274	580, 582, 588
	276, 288, 299	588, 594, 601
B-basis value (MPa)	219	539

and 1.8%. The average CAI strength (272 MPa) is approximately half of the NHC strength (583 MPa). Furthermore, the CAI strength exhibits considerable scattering. A two-parameter Weibull distribution function is applied for data reduction of the CAI and NHC strengths. [18,21,25–27]

$$F_f(S_f) = 1 - \exp\left\{-(S_f/S_0)^m\right\} \tag{1}$$

Therein, S_f, m and $S_{0,}$ respectively, denote the strength, Weibull shape, and scale parameters.

The Weibull plots of CAI and NHC strengths are depicted in Figure 3. The failure probability was calculated here using the so-called median rank method. The Weibull parameters were estimated using a maximum likelihood method (MLM). The following equations were solved numerically.[18,21]

$$\frac{n}{\hat{m}} + \sum_{i=1}^{n} \ln S_i - n\left(\sum_{i=1}^{n} S_i^{\hat{m}} \ln(S_i)\right) \Big/ \left(\sum_{i=1}^{n} \ln(S_i^{\hat{m}})\right) = 0$$

$$\hat{S}_0 = \left(\frac{1}{n}\sum_{i=1}^{n} S_i^{\hat{m}}\right)^{\frac{1}{\hat{m}}} \tag{2}$$

Therein, n denotes the sample size, S_i stands for the ith specimen strength, and $\hat{m}$ and $\hat{S}_0$, respectively, represent the maximum-likelihood estimates of the shape and scale parameters. The estimated values are presented in Table 1. The Weibull shape parameter for CAI strength ($m = 19.4$) is much lower than that for NHC strengths ($m = 61.8$), which implies that the considerable strength distribution is attributable to the variation in impact damage size.

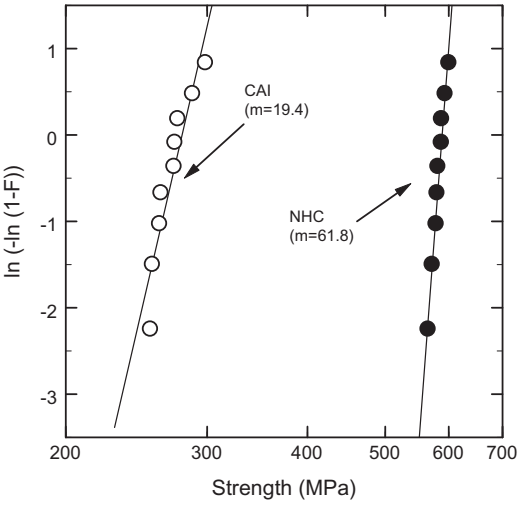

Figure 3. Weibull plots of CAI and NHC strengths (average strength: CAI 272 MPa, NHC 583 MPa).

Table 2. Experimental results of CAI fatigue tests*.

Minimum stress (MPa)	Weibull parameter		Fatigue exponent, b (=m/M)	Number of cycles to failure (lifetime)
	M	N_0		
200	0.74	1.83×10^6	26.2	126,365, 170,425, 353,353, 1,666,883 4,375,578, 6,287,444
210	0.76	6.11×10^5	25.6	26,522, 50,290, 126,760, 321,623, 552,690, 653,371, 950,782, 3,144,783
220	0.71	1.46×10^5	27.3	8967, 10,416, 17,279, 76,927, 80,120 97,426, 98,897, 456,465, 836,416
230	0.60	2.44×10^4	32.2	1175, 1923, 6198, 6710 84,230, 119,721
240	–	–		1407, 5840

*Stress ratio $R = S_{min}/S_{max} = 10$, frequency $f = 3$ Hz.

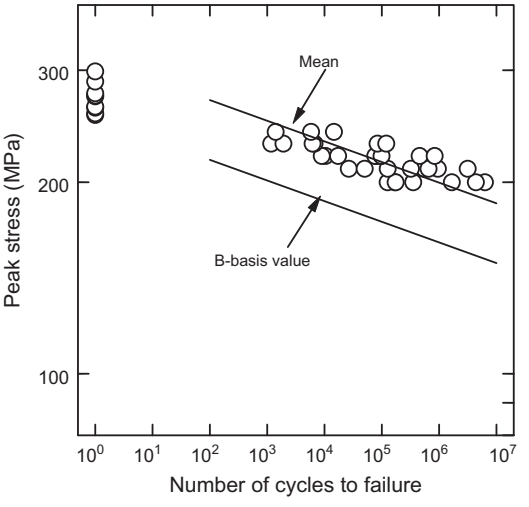

Figure 4. S–N curves of impact-damaged CFRP specimens under compression ($R = 10$, $f = 3$ Hz, impact energy = 6.7 J/mm).

3.2. CAI fatigue strength distributions

The experimentally obtained results of CAI fatigue tests for impact-damaged CFRP specimens under cyclic compression are presented in Table 2. and the S–N data are presented in Figure 4 . The fatigue failure mode was the same as that of compressive testing. CAI fatigue lifetime exhibits flat S–N curves and considerable scattering. Fatigue failures occurred under fatigue testing conducted at the 73% of CAI strength, which agrees with the data described in some reports.[1–18] Weibull statistics were adopted for fatigue lifetime distribution under the same peak compressive stress S_{min}.[11,18,21]

$$F_f(N_f) = 1 - \exp\{-(N_f/N_o)^M\} \tag{3}$$

In that equation, N_f represents the fatigue lifetime, and M and N_0 are the Weibull shape and scale parameters. Weibull plots showing fatigue lifetime distributions for 200, 210, 220, and

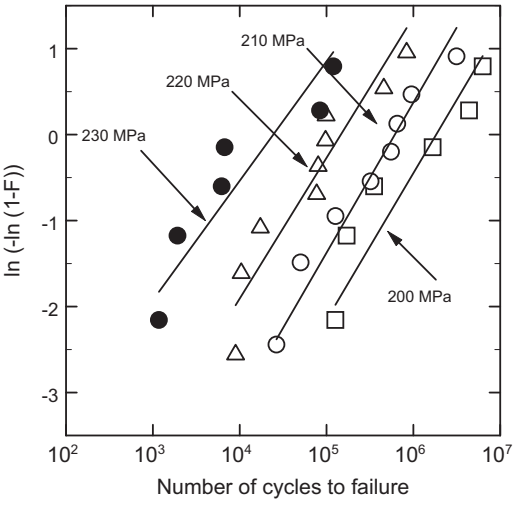

Figure 5. Weibull plots of CAI fatigue lifetime distribution. Weibull parameters were estimated using MLM. ($R = 10$, $f = 3$ Hz, impact energy = 6.7 J/mm).

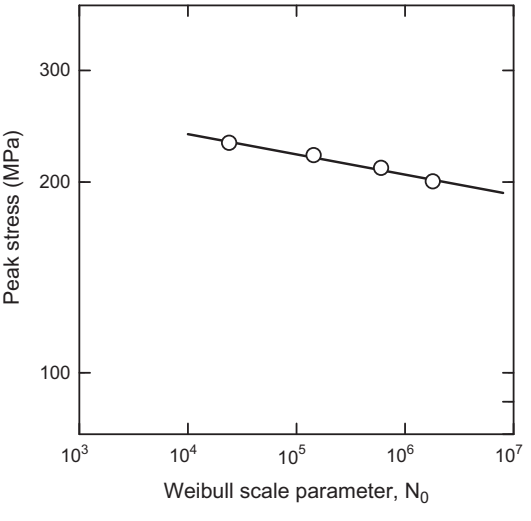

Figure 6. Peak compressive stress and Weibull scale parameter N_0. The fatigue exponent b is estimated as 31.

230 MPa are presented in Figure 5. The Weibull shape parameters (M) estimated using MLM are 0.74, 0.76, 0.71, and 0.60 for 200, 210, 220, and 230 MPa, which are apparently independent of the stress. Using a joint Weibull method,[18] the common shape parameter was estimated as 0.702.

Figure 6 presents a double logarithmic plot of Weibull scale parameters (N_0) vs. peak compressive stress ($S_{\min}$). The following relationship between Weibull scale parameters (N_0) and peak compressive stress ($S_{\min}$) was ascertained empirically.[21]

$$N_0 = (S_{\min}/K)^{-b} \tag{4}$$

Therein, b and K are constants. The value of b, which is often designated as a fatigue exponent, was estimated as 30.8. The fatigue exponent b for smooth specimens of aluminum alloy is generally less than 10.[28] The large fatigue exponent value suggests that the damage growth of CFRP under cyclic compressive loading is extremely sensitive to stress.

Jones et al. reviewed some experimentally obtained results for S–N curves of damaged laminates in 1987[7] and concluded that the S–N curves have a generic shape with a pronounced threshold level. However, the pronounced fatigue limit has not been observed in this study because of the difference in the material constituents. The interleaf layer, in which thermoplastic particles are dispersed, is applied for the material used for this study. The viscoplastic/viscoelastic properties of the epoxy matrix must differ greatly from those of primitive epoxy resin developed during the 1980s.

3.3. *Damage growth behavior*

The damage growth behavior was evaluated using ultrasonic C-scanning for a specimen tested at $S_{min} = 220$ MPa, $R = 10$, $f = 3$ Hz. Specimens were inspected using reflection mode, and the frequency of the ultrasound transducer was 10 MHz. Typical C-scan images at 0, 10^5, and 10^6 cycles are shown in Figure 7. Damage growth is not clearly visible until 10^6 cycles, although the lifetime was 1.23×10^6. The pulse-echo intensity from damage seems to increase with the number of cycles, which implies that the residual opening displacement of delamination increases with cyclic loading.

Photographs obtained from a digital video recording, showing the damage growth of a specimen tested at $S_{min} = 200$ MPa, $R = 10$, $f = 3$ Hz, are presented in Figure 8. Damage growth in the transverse direction was observed very close to the end of the specimen lifetime (1000–1500 cycles) before the final failure (1.67×10^6). Until then (more than 1.67×10^6 cycles), no visible damage growth was observed. This damage growth starts very close to the end of the specimen lifetime. The experimentally obtained results agree with data reported from earlier studies.[1,3,6,12]

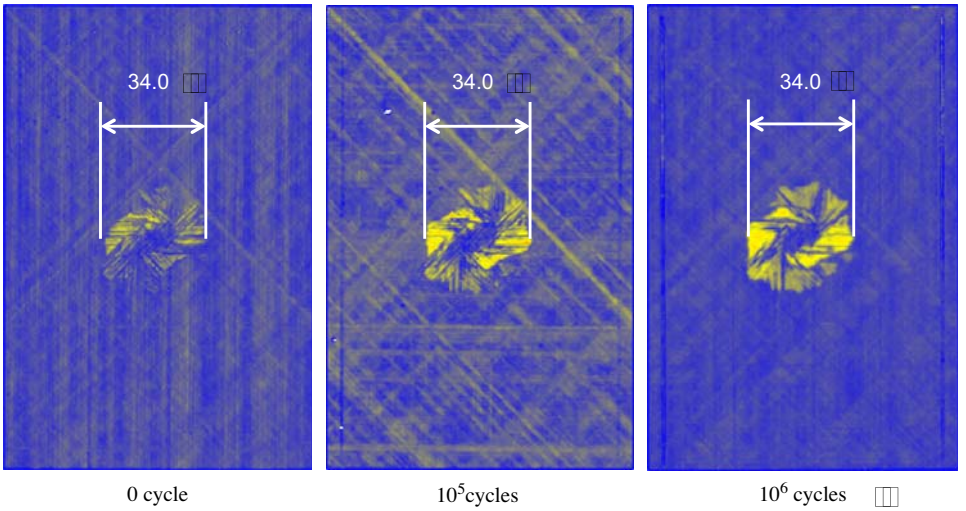

Figure 7. Ultrasonic C-scan images showing damage growth after cyclic compressive loading ($S_{min} = 220$ MPa, $R = 10$, $f = 3$ Hz, fatigue life 1.23×10^6).

Figure 8. Observations of damage growth using digital video recording ($S_{min} = 200$ MPa, $R = 10$, $f = 3$ Hz, fatigue life 1.67×10^6).

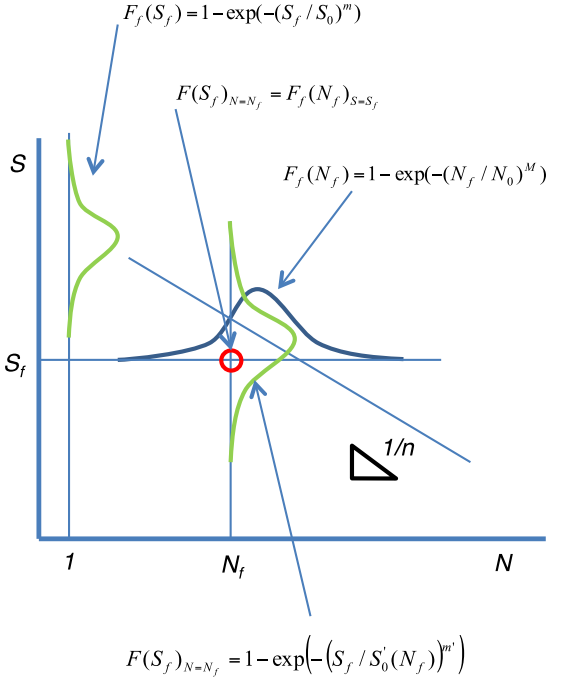

Figure 9. Schematic drawing showing the relationship between residual strength and fatigue lifetime distributions.

3.4. *Relationship between CAI strength and fatigue lifetime distributions*

Figure 9 presents a schematic diagram depicting the relationship between CAI strength and fatigue lifetime distributions. We assumed a one-to-one correspondence between CAI strength and the fatigue lifetime. If the number of cycles to failure is N_f under the minimum stress S_{min}, then we assumed the strength probability at N_f is identical to the fatigue probability at $S = S_{min}$.

$$F_f(S_{min})_{N=N_f} = F_f(N_f)_{S=S_{min}} \tag{5}$$

Substituting Equations (1), (3), and (4) into Equation (5) yields the strength distribution at the number of cycles of N_f.

$$F_f(S_f)_{N=N_f} = 1 - \exp\{-(S_f/S_o')^{m'}\}$$
$$m' = bM \quad S_o' = KN_f^{-1/b} \tag{6}$$

Consequently, a simple relationship between the Weibull shape parameter of fatigue lifetime, M and that of CAI strength m' is obtained. In this study, the Weibull shape parameters m' estimated from the total shape parameter of fatigue M (=0.702) and b (=30.8) is 21.6. This value is almost identical to the Weibull shape parameter m for the initial CAI strength distribution (=19.4). The result suggests that the fatigue lifetime distribution is attributable mainly to the initial CAI strength distribution.

Tomblin and Seneviratne investigated the CAI fatigue behavior of Cytec AS4/E7K8 plain-weave fabric composite and conducted statistical analyses based on Weibull statistics.[18] Regardless of the feature of fiber reinforcement, the CAI fatigue behavior is thought to be almost same because the CAI fatigue is strongly affected by the delamination due to impact loading. The estimated Weibull shape parameters are presented in Table 3. The Weibull shape parameters of fatigue life, M, were estimated using the 'Joint Weibull Method'. The Weibull shape parameter, m, of 25/50/25 BVID specimens is apparently incorrect. Therefore, the corrected value calculated by the author from raw data is presented in this table. The fatigue exponents, b, were estimated using Equation (4) $(N_0 = (S_{\min}/K^{-b})$, and Equation (6) $m = bM$ under the assumption of $m = m'$. Except for the 40/20/40 VID specimens, the fatigue exponent b estimated from the slope in $\ln(S_{\min})$ vs. $\ln(N_0)$ diagram are close to that estimated from Weibull shape parameters of the static strength and fatigue lifetime. Of course, the sample size is insufficient to carry out statistical analyses because only 5–6 specimens were examined in their work. The result suggests that a one-to-one correspondence between the static strength and the fatigue lifetime is reasonable.

This relationship might be useful to reduce the number of specimens for determining the B-basis value of fatigue strength. Generally, a few tens of specimens are tested under each stress level to ascertain the slope in an S–N curve, which implies that more than several tens of specimens are required. If the number of specimens is insufficient, then the estimated fatigue exponent, b (inverse of the slope in SN curve) is not reliable because CFRP exhibits a flat S–N curve as the slope as compared with aluminum alloys. Using the relationship shown in Equation (6), the fatigue exponent b can be estimated from the Weibull shape parameter of strength m and that of fatigue M. It is not necessary to conduct fatigue tests while varying the applied stress level, which substantially reduces the related costs and time. However, it is noteworthy that this method is not applicable to fatigue data reduction of specimens without initial damage. The fatigue behavior of composites without initial damage is known to be generally complicated. Various instances of damage such as matrix cracking, delamination, and fiber breakage occur simultaneously and/or sequentially. [29] In this case, one-to-one correspondence between the static strength and the fatigue lifetime cannot be assumed.

Finally, the procedure to determine a design allowable level (B-basis value) is described for convenience. The B-basis value of the Weibull distribution is generally given by the following equations [20,27] as

Table 3. Weibull shape parameter and fatigue exponent of Cytec AS4/E7K8 plain-weave fabric composite (data are referred from Ref. [18]).

		Weibull shape parameter		Fatigue exponent, b	
Lay-up[a](0°/±45°/90°)	Impact damage[b]	CAI strength, m	Fatigue life, M[d]	$b = m/M$	Slope of ln S_{min} vs. lnN_0
10/80/10	VID	49.4	2.78	17.8	24.3
25/50/25	VID	32.2	2.78	11.6	19.2
25/50/25	BVID	52.4[c]	2.36	22.2	25.8
40/20/40	VID	33.0	3.69	8.9	20.6

[a]Lay-up percentages of 0°, ±45°, and 90° layers, respectively.
[b]VID; visible impact damage, BVID; barely visible impact damage.
[c]The Weibull shape parameter reported in Ref. 18 is apparently wrong. This value was calculated using authors from the raw data.
[d]Weibull shape parameters of fatigue life were estimated using the 'Joint Weibull Method'.

$$B = \hat{q}\exp\{-V_B/(\hat{m}\sqrt{n})\}$$
$$\hat{q} = \hat{S_o}(-\ln(0.9))^{1/\hat{m}}, \tag{7}$$

where n represents the sample size, and where $\hat{m}$ and $\hat{S}_0$, respectively, denote the maximum-likelihood estimates of the shape and scale parameters in Equation (1) and (6). V_B is a one-sided B-basis tolerance factor for the Weibull distribution. An approximation to the V_B values is given as follows [20]:

$$V_B \approx 3.803 + \exp\{1.79 - 0.516\ln(n) + 5.1/(n-1)\} \tag{8}$$

Although fatigue exponent b includes statistical scattering, b is assumed to be constant for simplicity in this study. The estimated B-basis values are superimposed on Figure 4. The ratios between the endurance limit at 10^6 and 10^7 cycles and the initial static strength (219 MPa) were estimated as 0.74 (161 MPa) and 0.68 (149 MPa), respectively, which implies that the degradation caused by cyclic compressive loading ($R = 10$) is not negligible for impact-damaged composite laminates. The S–N curve of impact-damaged laminates depends strongly on the specimen size. The CAI fatigue test configuration in accordance with ASTM D7136 and D7137 provides a much worse case of strength degradation than that with actual aircraft structures.

4. Conclusion

Fatigue lifetime data of impact-damaged carbon fiber/toughened epoxy composites under compressive loading were obtained to elucidate fatigue behavior and statistical characteristics. The following conclusions were made:

- Fatigue lifetime data of impact-damaged carbon fiber/epoxy composites (Impact energy 6.7 J/mm) were obtained. The total number of specimens was 31.
- The CAI strength and fatigue lifetime exhibit considerable scattering. This result is apparently derived from the variation in impact damage size.
- The ratios between the endurance limit at 10^6 and 10^7 cycles and the initial static strength were estimated respectively as 0.74 and 0.68.
- A simple statistical model was proposed for predicting the lifetime of impact-damaged CFRP laminates. In spite of rough approximation, the estimates agreed with the experimentally obtained results.

Acknowledgements

The authors wish to thank Mr. Takashi Yamazaki and Dr. Eiichi Hara of IHI Jet Service Co. Ltd. for their assistance with fatigue experiments.

References

[1] Polymer matrix composites: materials, usage, design and analysis, the composite materials handbook (MIL 17–3F), Volume 3. West Conshohocken (PA): ASTM International; 2002. Chapter 7.7, Damage growth under cyclic loading; p. 7-58–7-60.

[2] Ramkumar RL. Compression fatigue behavior of composites in the presence of delaminations. In: Reifsnider K, editor. Damage in composite materials. Philadelphia (PA): ASTM STP 775; 1982. p. 184–210.
[3] Ramkumar RL. Effect of low-velocity impact damage on the fatigue behavior graphite/epoxy laminates. In: O'Brien TK, editor. Long-term behavior of composites. Philadelphia (PA): ASTM STP 813; 1983. p. 116–135.
[4] O'Brien TK. Interlaminar fracture of composites. Hampton (VA): NASA TM-85768; 1984.
[5] Demuts F, Whitehead RS, Deo RB. Assessment of damage tolerance in composites. Compos. Struct. 1985;4:45–58.
[6] Clark G, Van Blaricum TJ. Load spectrum modification effects on fatigue of impact-damaged carbon fibre composite coupons. Composites 1987;18:243–251.
[7] Jones R, Williams JF, Tay TE. Is fatigue testing of impact damaged laminates necessary? Compos. Struct. 1987;8:1–12.
[8] Nyman T. Composite fatigue design methodology: a simplified approach. Compos. Struct. 1996;35:183–194.
[9] Beheshty MH, Harris B. A constant life model of fatigue behavior for carbon-fibre composites: the effect of impact damage. Compos. Sci. Technol. 1998;58:9–18.
[10] Beheshty MH, Harris B, Adam T. An empirical fatigue-life model for high-performance fibre composites with and without impact damage. Composites Part A 1999;30:971–987.
[11] Tai NH, Ma CCM, Lin JM, Wu GY. Effect of thickness on the fatigue behavior of quasi-isotropic carbon/epoxy composites before and after low energy impacts. Compos. Sci. Technol. 1999;59:1753–1762.
[12] Mitrovic M, Hahn HT, Carman GP, Shyprykevich P. Effect of loading parameters on the fatigue behavior of impact damaged composite laminates. Compos. Sci. Technol. 1999;59:2059–2078.
[13] Melin LG, Schön J. Buckling behavior and delamination growth in impacted composite specimens under fatigue load: an experimental study. Compos. Sci. Technol. 2001;61:1841–1852.
[14] Melin LG, Schön J, Nyman T. Fatigue testing and buckling characteristics of impacted composite specimens. Int. J. Fatigue 2002;24:263–272.
[15] Symons DD, Davis G. Fatigue testing of impact-damaged T300/914 carbon-fibre-reinforced plastic. Compos. Sci. Technol. 2000;60:379–389.
[16] Gower MRL, Shaw RM. ECCM 13 conference proceedings, 2–5 June 2008. Sweden: Stockholm; 2008.
[17] Uda N, Ono K, Kunoo K. Compression fatigue failure of CFRP laminates with impact damage. Compos. Sci. Technol. 2009;69:2308–2314.
[18] Tomblin J, Seneviratne W. Determining the fatigue life of composite aircraft structures using life and load-enhancement factors, DOT/FAA/AR-10/6. Washington (DC): Federal Aviation Administration (FAA), US Department of Transportation; 2011.
[19] Advisory Circular AC 20–107A. Composite aircraft structure. Washington (DC): Federal Aviation Administration; 1984.
[20] Polymer matrix composites: materials, guidelines for characterization of structural materials, the composite materials handbook (MIL 17–3F), Volume 1. West Conshohocken (PA): ASTM International; 2002. Chapter 8, Statistical methods; p. 8-1–8-109.
[21] Hahn HT, Hwang DG. Fatigue behavior of composite laminates. Technical Report, AFWAL-TR-80-4172, Wright–Patterson Air Force Base; 1980.
[22] ASTM D7136/D7136M-12. Standard test method for measuring the damage resistance of a fiber-reinforced polymer matrix composite to a drop-weight impact event. West Conshohocken (PA).
[23] ASTM D7137/D7137M-12. Standard test method for compressive residual strength properties of damaged polymer matrix composite plates. West Conshohocken (PA).
[24] ASTM D6641/D6641M-09. Standard test method for compressive properties of polymer matrix composite materials using a combined loading compression (CLC) test fixture. West Conshohocken (PA).
[25] Gathercole N, Reiter H, Adam T, Harris B. Life prediction for fatigue of T800/5245 carbon-fibre composites: I constant amplitude loading. Fatigue 1994;16:523–532.
[26] Whitney JM. Fatigue characterization of composites materials. In: Lauraitis KN, editor. Fiber composites materials. Philadelphia (PA): ASTM STP 723; 1981. p. 133–151.
[27] Barbero EJ, Gutierrez JM. Determination of basis values from experimental data for fabrics and composites. SAMPE 2012 Conference and Exhibition, Baltimore; 2020 May 21–24. Covina (CA).

[28] Suresh S. Fatigue of materials. Cambridge University Press; Cambridge; 1991, Chapter 4, Phenomenological approaches based on cyclic stress and cyclic, strain, p. 126–140.
[29] Reifsnider KL, Schulte K, Duke JC. Long-term fatigue behavior of composite materials. In: O'Brien TK, editor. Long-term behavior of composites. Philadelphia (PA): ASTM STP 813; 1983. p. 136–159.